

# Thermophysical properties of polypentadecanolactone

P. Skoglund and Å. Fransson\*

Department of Applied Physics and Electronics, Umeå University,  
 SE-901 87 Umeå, Sweden  
 (Received 1 January 1997)

In this paper we present thermodynamic properties and crystallization kinetics of the aliphatic polyester, polypentadecanolactone, with largely unknown properties. Experimental specific heat capacity values, melting and glass transition characteristics are analysed, as are the crystallization processes during different conditions. Equilibrium melting temperatures are deduced with the Hoffman-Week extrapolation method. The overall crystallization kinetics are analysed with the Avrami equation, and the Lauritzen-Hoffman crystallization theory is applied to the data. © 1998 Elsevier Science Ltd. All rights reserved.

(Keywords: polypentadecanolactone; crystallization; segregation)

## INTRODUCTION

The interest in aliphatic polyesters has grown rapidly since the discovery of the biodegradable and non-toxic polymers such as, polycaprolactone (PCL). Accordingly, a large number of possible technical implementations have been proposed for PCL and its relatives<sup>1–4</sup>. The rather low melting temperature for PCL of about 325 K<sup>5</sup> may however limit its practical applications. Higher polylactones, with a larger number of ethylene units between the COO groups, have higher melting temperatures and can therefore in some cases be more suitable. The properties of these higher polylactones are, however, largely unknown. In this paper, we investigate polypentadecanolactone (PPDL) with structure formula  $-(\text{CH}_2)_{14}\text{COO}-$ . Compared to PCL, this polymer is expected to behave more like polyethylene due to the reduced importance of the COO groups. The purpose of this work is to present important thermodynamic properties such as specific heat capacity, glass and melting transition data. Further, we investigate the crystallization kinetics and the influence from the crystallization procedure on the material characteristics.

## EXPERIMENTAL

### Methods

A Perkin-Elmer Differential Scanning Calorimeter (DSC-2), equipped with the intracooler II cooling system and with nitrogen as a purge gas, was used at the experiments. The low temperature measurements were done with liquid nitrogen as a coolant and neon as purge gas. Unless otherwise mentioned, melting and crystallization temperatures are defined as the intersection point of the baseline with the leading edge of the crystallization or melting curve.

The glass transition temperature is taken at the point where the shift in specific heat capacity is halfway between the glassy and liquid states. Melting and crystallization enthalpies were deduced according to methods described

by Richardson<sup>6</sup>, and the temperature calibration on cooling has been described by us elsewhere<sup>7</sup>. The microscopic observations were done with a Nikon polarizing microscope.

### Material

The investigated polypentadecanolactone sample was kindly supplied by Professor B. V. Lebedev at the Lobachevsky State University, Nizhny Novgorod, Russia. The sample has the following characteristics. Elemental composition (in mass%): carbon 75.44 where 74.95 is the stoichiometric value, hydrogen 11.69 compared to the calculated 11.74 and, finally, oxygen 12.87 compared to 13.31. The intrinsic viscosity is 0.20 dl/g, in chloroform at 298 K. The polymer was analysed by Polymer Source Inc., Dorval, Canada with Gel Permeation Chromatography (GPC), with the following result. The molecular number average was 5500, the molecular weight average 19 400 and the  $z$ -average 48 300, with a polydispersity of 3.53. A sample with mass 6.29 mg was encapsulated in a standard aluminium pan, and no mass loss was detected after the experiments.

## RESULTS AND DISCUSSION

In *Figure 1* we show the mean values of three independent measurements of the specific heat capacity ( $c_p$ ) in the temperature region 115–140 K. The data were found after cooling from 400 K in the melt, with 40 K/min to 110 K and after a 10 min annealing at 110 K. The measurements were then taken at a heating rate of 10 K/min. After this treatment, we find a broad glass transition between 235 K and 270 K, as seen in the inset plot in *Figure 1*, with a transition temperature ( $T_g$ ) close to 250 K. The shift in specific heat capacity at  $T_g$  is about 0.1 J/g K. Lebedev and Yevstropov<sup>8</sup> who made adiabatic measurements report a  $T_g$  of 251 K on a sample with intrinsic viscosity of 0.93 dl/g in chloroform at 298.15 K, revealing a sample of higher molecular weight. After the heat treatment described above, we get a melting temperature ( $T_m$ ) of about 355 K, while the

\* To whom correspondence should be addressed

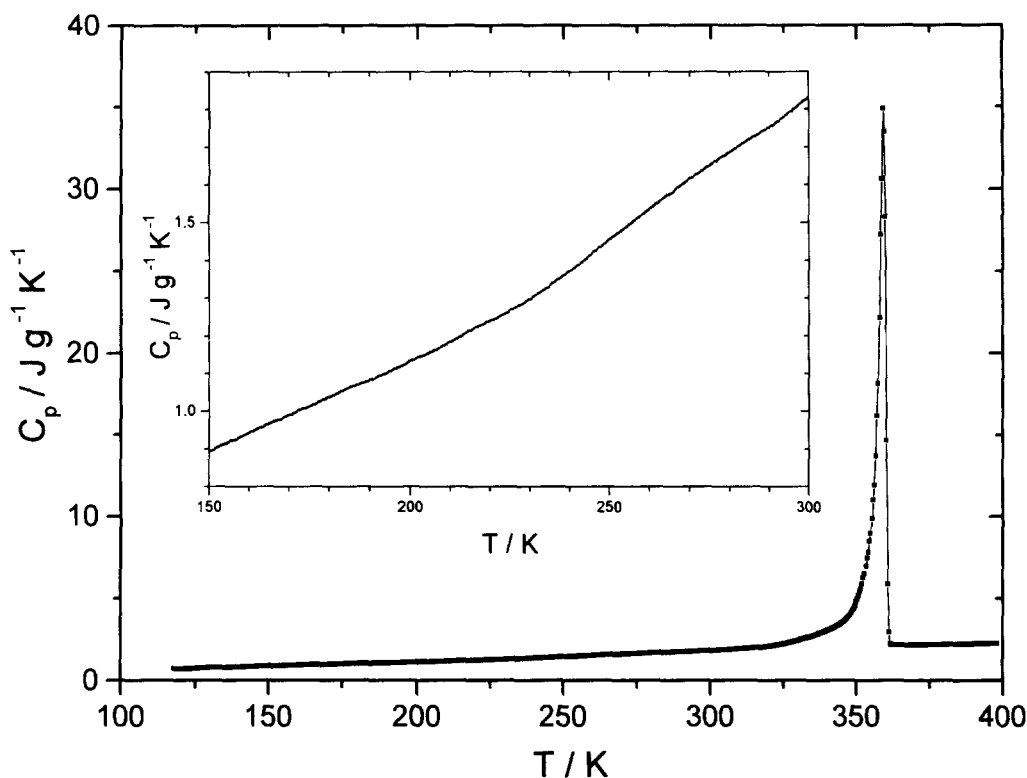


**Figure 1** Specific heat capacity versus temperature for PPDL. Inset plot shows the broad glass transition at 250 K

peak temperature is 359 K. The corresponding melting enthalpy ( $\Delta h_m$ ) at 355 K is about 153 J/g, while equilibrium crystals are reported to have a melting enthalpy of 233 J/g<sup>8</sup> and 263.7 J/g<sup>9</sup> at an equilibrium melting point of 370.5 K. In our case, the melting starts at temperatures close to 327 K and ends at 362 K, although the main melting (71%) occurs in a narrow temperature interval between 350 and 362 K. Further, we find that the  $c_p$  values below  $T_g$  and above  $T_m$  agree well with those reported by Lebedev and Yevstropov<sup>8</sup> and by the Wunderlich group<sup>9</sup>. Our  $c_p$  data are about 0.04 J/g K higher than the calculated values of Wunderlich *et al.* below  $T_g$  and 0.02 J/g K higher above  $T_m$ . The deviation from the adiabatically determined  $c_p$  by Lebedev and Yevstropov are even smaller, showing that the discrepancies are well within the experimental error. The relatively low molecular weight of the sample investigated here, combined with its polydispersity means that the fractionation into crystals of different melting points, may be substantial. The premelting effect shows that crystals of different quality are present<sup>10</sup>.

#### Hoffman-Week equilibrium melting point

We determined the equilibrium melting point by the Hoffman-Week extrapolation method, where the melting points are plotted as a function of the isothermal crystallization temperature ( $T_c$ ), according to equation (1)<sup>11</sup> below:

$$T_m = T_m^\circ \left(1 - \frac{1}{\beta}\right) + \frac{T_c}{\beta} \quad (1)$$

Here  $T_m$  is the experimental melting point,  $T_m^\circ$  is the equilibrium melting temperature and  $\beta$  is proportional to the ratio of the lamellar thickness to the thickness of the initial nucleus at  $T_c$ . Experimental parameters such as heating rate and time of crystallization are affecting the observed melting points, and the lamellar thickening rate is assumed to be proportional to the crystallization rate. Therefore the time of

crystallization must be associated with the crystallization rate at every  $T_c$ . The time dependency of the  $\beta$  parameter is strong at the initial stages of the crystallization. We have therefore chosen a crystallization time as three times the half crystallization time ( $t_{1/2}$ ), i.e. three times the time needed to obtain 50% conversion. In *Figure 2* we show melting temperatures, defined by the end tail of the melting interval ( $T_{m, \text{end}}$ ), of samples crystallized for  $3t_{1/2}$  at various  $T_c$ . Extrapolation of the fitted line to  $T_m = T_c$  gives a Hoffman-Week equilibrium melting temperature of about 370 K. The slope of the fitted line is 0.38 which corresponds to a  $\beta$  value of 2.6. The extrapolation of  $T_m$  is only valid if  $\beta$  is constant. Literature data on the related polymer PCL show that some of the differences in the extracted  $T_m^\circ$  values are caused by the experimental procedures. Phillips *et al.*<sup>12</sup> investigated three PCL samples with molecular weight averages ( $M_w$ ) of 7000, 15000 and 40000 with polydispersity 1.5–2, using a hot stage microscopy. Data collected at a heating rate of 10 K/min, showed that the slopes or  $\beta$ -values really depend on the crystallization time at  $T_c$ . A linear relation between  $T_m$  and  $T_c$  is normally found at the relatively high crystallization temperatures. At short crystallization times, Phillips *et al.* show not only lower melting temperatures but also a non-linear relation between  $T_m$  and  $T_c$ . However, using only the higher crystallization temperatures they found a linear relation of  $T_m$  versus  $T_c$  even for the shortest crystallization times, although with a considerably steeper slope compared to the long time crystallization case. This linear part of the short crystallization time case were extrapolated to the same equilibrium melting temperature as the long time crystallization case. The long time crystallization, corresponding to a large thickening of the crystals, gives however a more reliable extrapolation according to the authors. Phillips *et al.* found that  $T_m^\circ$  increased slightly with  $M_w$ , and was found to be 341.0 K, 342.5 K and 343.5 K,

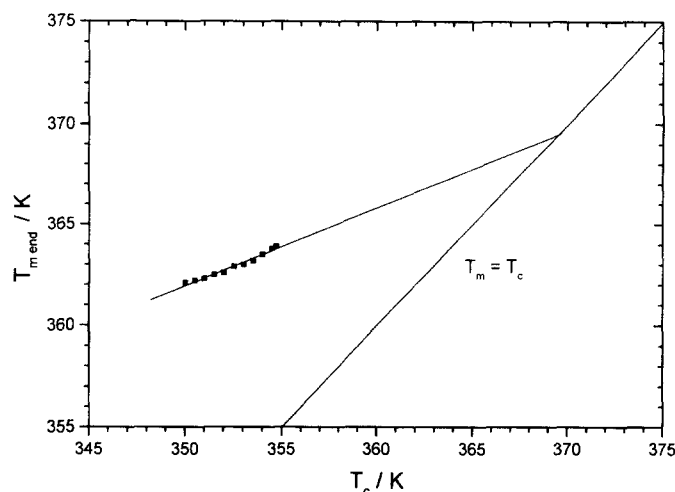


**Figure 2** Melting points as a function of crystallization temperature. All measurements were taken at a heating rate of 5 K/min. Equilibrium melting point is found at the intersection of the lines according to Hoffman-Week extrapolation method

respectively. De Juana and Corta'zar<sup>13</sup> investigated a PCL sample with  $M_w = 17\,600$  and  $M_n = 10\,800$ , and found from DSC data a  $T_m^\circ$  of 332.3 K. In their experiment, they used the onset value of the melting peak at 10 K/min as the melting point, and the crystallization time was set to the time needed to reach 10% of the final crystallinity. Hot stage microscopy on the same material at 3 K/min, and with the midpoint of the transition taken as the melting point gave a  $T_m^\circ$  of 336.7 K. They interpreted the difference in  $T_m^\circ$  as an effect of different definitions of the melting points. Goulet and Prud'homme<sup>14</sup> found an equilibrium melting temperature of 347 K from DSC data at a heating rate of 20 K/min on a PCL sample of  $M_w = 48\,000$  and polydispersity 1.1. They used the end of the melting interval as melting point, and the crystallization times were set to  $5t_{1/2}$ . The different molecular weights for the various PCL samples discussed above cannot explain the differences in the equilibrium melting points, so the choice of experimental procedure is important. This is also discussed in a study on a broad molecular weight distribution of polyethylene with  $M_w = 80\,000$ , reported by Wunderlich<sup>15</sup>. He shows that for melting temperatures defined by the initial part of the melting peak and by the peak temperature itself, annealing effects in particular for the lower crystallization temperatures. Melting temperatures defined by the end tail gave, on the contrary, a straight line of  $T_m$  versus  $T_c$ . These melting temperatures, which are the melting temperatures of the thickest crystals, usually give a more reliable extrapolation. The above comparison of equilibrium melting temperatures shows that there is a considerable sensitivity of the Hoffman-Week  $T_m^\circ$  both to the crystallization time and the definition of the melting temperature. If we return to PPDL, Lebedev and Yevstropov<sup>8</sup>, who made adiabatic measurements, give an equilibrium melting temperature of 370.5 K, which is in good agreement with our value of 370 K. They used a method based on plotting the temperature versus the inverse of the melted fraction, where the slope of the plot corresponds to the melting point depression which is caused by the non-ideal crystals.

#### *Isothermal and continuous cooling crystallization*

The sensitivity of crystallization characteristics to annealing times is obvious in *Figure 3*. The selected melting endotherms correspond to crystallization times ranging from 4 min to 74 h, all at  $T_c = 352$  K. The increase

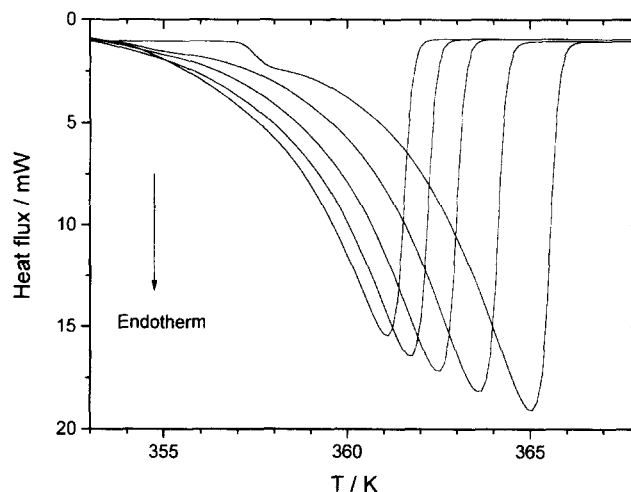


**Figure 3** Melting peaks of PPDL at a heating rate of 5 K/min and found after increasing annealing times at 352 K. From the left to the right, the annealing times are 4, 16, 64, 426 and 4440 min

in the observed  $T_{m, \text{end}}$  and  $\Delta h_m$  with crystallization time is apparent in *Figure 4*. As can be seen, with the increase in melting temperature for increasing crystallization times follows an increase in the heat of melting, due to further crystallization and perfection of initially poorly crystallized macromolecules. This so-called secondary crystallization is substantial and the measured melting enthalpy increases from 86 to 112 J/g when the crystallization time increases from 4 min to 74 h. The secondary crystallization does normally not follow the Avrami expression as discussed below, but has usually a logarithmic time dependency for some time—decades before it finally ceases<sup>10</sup>. If  $T_c$  is lowered by 2 K to 350 K and the crystallization time is kept at 74 h, the melting enthalpy is further increased to 131 J/g, although the  $T_{m, \text{end}}$  value is just slightly lower (365.8 K) than the value 366.3 K found at  $T_c = 352$  K. This indicates that the increase in melting enthalpy on decreasing  $T_c$  is mainly due to a larger fraction of crystallized material and not due to higher crystal perfection, which would give a higher  $T_{m, \text{end}}$ . The results show that even after extended crystallization times only some of the molecules in the sample, i.e. the larger molecules, are able to crystallize at the two given isotherms. This segregation of the molecules

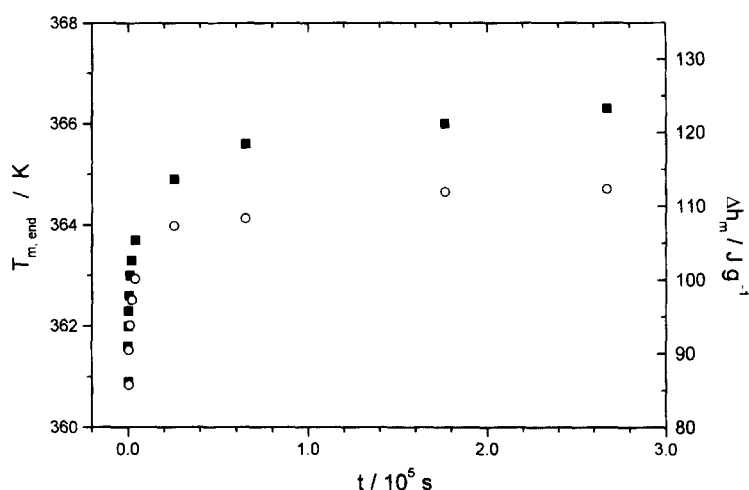


**Figure 4** The end temperature of the melting peaks (filled squares and left scale) and the melting enthalpies (open circles and right scale) found after increasing annealing times from 4 to 4440 min at 352 K

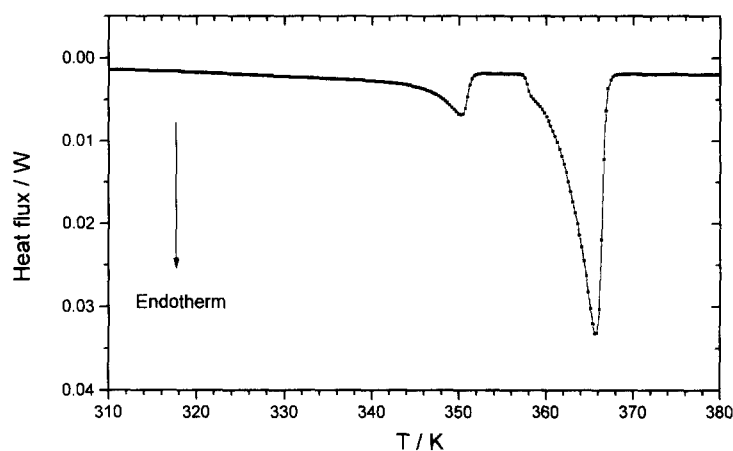


**Figure 5** Dual melting peaks found after isothermal crystallization at 352 K for 4440 min followed by cooling to 300 K with 80 K/min. The measurements were then taken at a heating rate of 10 K/min

depends on the time available for crystallization. After isothermal crystallization at 352 K and a rapid cooling to 300 K, we find double melting peaks on heating. In *Figure 5* we show the heating scan found after 74 h of crystallization at 352 K. The area under the high temperature melting peak has its source in the material isothermally crystallized at 352 K, and the low temperature peak to that crystallized during the subsequent cooling to 300 K. The high temperature peak increases with the crystallization time at 352 K, from about 90 J/g after 4 min to an almost stable value of the order 118 J/g found after 74 h. This is in good agreement with the melting enthalpies found after heating of the material crystallized at 352 K at the corresponding annealing times, and presented in *Figures 3 and 4*. The total area under the melting peaks is about 150–155 J/g, which is close to the value of the single peak in *Figure 1*. We conclude that about 75% of the apparent total crystallizable mass are able to crystallize at 352 K. If the experiment is repeated at a higher crystallization temperature of 355 K, we find an even more pronounced segregation and the low temperature melting peak becomes now larger. Also in these cases, the area under the high temperature peak increases with the time at  $T_c = 355$  K, but the total heats of melting are still close to 155 J/g, mainly independent of the time at  $T_c$ . After 74 h of annealing at 355 K, the area under the high

temperature peak, originating from the material crystallized at 355 K, has a melting enthalpy of 81 J/g. This kind of fractionation into different crystals was explained by Wunderlich<sup>10</sup>, who introduced the concept molecular nucleation. By this means the initial organization of the first part of a macromolecule in the crystalline phase. According to this concept, where the effect of chain ends is incorporated, there exists a critical molecular weight ( $M_c$ ) at each  $T_c$ , where only molecules with molecular weights higher than  $M_c$  are able to crystallize. Thus, each molecule must be large enough to create a stable nucleus, and the shorter molecules can only crystallize on further cooling. In *Figure 6* we show the progress of the isothermal crystallization process at temperatures between 352 and 356 K. The lowest temperature is here limited by the rapid crystallization of the PPD L sample, which makes the analysis unreliable at temperatures lower than 352 K. The agreement between the apparent final (primary) isothermal crystallization enthalpy of 85 J/g at 352 K and the result from the melting peaks found after the corresponding annealing time in *Figure 4*, shows that no major rearrangement of the molecules occurs during the comparably short time period of the heating scan. However, the relatively low released heat compared to the melting enthalpy found after longer times of annealing, as seen in *Figure 4*, and that

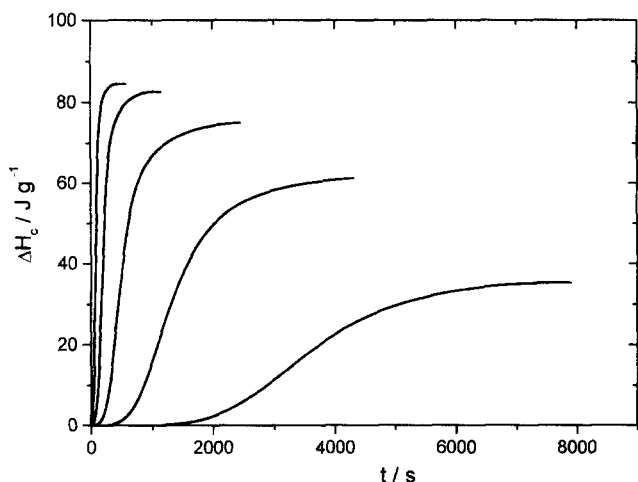


**Figure 6** Isothermal crystallization enthalpy versus time. Isotherms are increasing from 352 K to 356 K with 1 K from left to right

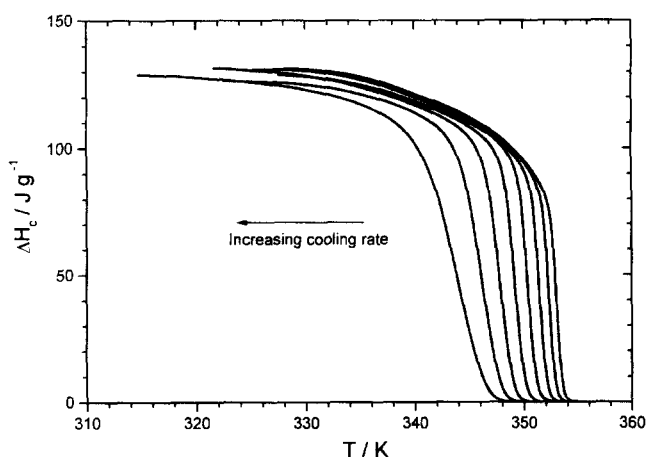


**Figure 7** Continuous cooling crystallization enthalpy versus temperature. Cooling rates are increasing from 0.31 to 40 K/min from right to left, doubled in each step

obtained from the melting peak in *Figure 1*, shows that the crystallization process will proceed further if the temperature is lowered and/or the time is increased. As discussed earlier in connection with *Figures 4 and 5*, we interpret the remaining differences of crystallized material, found after extended time periods at different crystallization temperatures, as a result of the rather low molecular weight of this sample in combination with the polydispersity which will enhance the segregation. The results from the continuous cooling experiments show substantial higher crystallization enthalpies of approximately 130 J/g, and mainly independent of cooling rates. The features are shown in *Figure 7*. As the cooling rate increases, the crystallization temperatures decrease from 354.0 to 347.9 K. The apparent decrease of the conversion rate at the lowest cooling rate, here observed at about 85 J/g and 351.5 K, is interpreted as a consequence of the segregation effect. The number of molecules that are able to crystallize at these temperatures reduces rapidly and the conversion rate will thus decrease. The cooling rate is too low to support enough of crystallizable species. This effect is not seen for the higher cooling rates where the sample is cooled rapidly enough to keep up the number of crystallizable molecules. The point where the deviation is found agrees well with the apparent final isothermal crystallization enthalpy at 352 K found in

*Figure 6*. However, it is noticed that the slow secondary crystallization will increase the conversion degree if the cooling is stopped, as discussed in connection with *Figure 4*.

#### Overall kinetics of crystallization

In the further analysis of the overall crystallization kinetics we apply the Avrami equation to the primary isothermal crystallization:

$$1 - X(t) = \exp(-kt^n) \quad (2)$$

where  $X$  is the crystalline fraction,  $t$  the time and  $n$  the Avrami exponent. For three dimensional spherulitic growth, the theory predicts an  $n$  value of 3 if the nucleation is athermal and a value of 4 for sporadic or thermal nucleation. Finally,  $k$  is the rate constant, depending both on the nucleation and growth rates. The equation above is usually linearized as follows:

$$\ln[-\ln\{1 - X(t)\}] = \ln(k) + n\ln(t). \quad (3)$$

If the crystallization follows the Avrami theory, then straight lines should be found in plots of data according to equation (3). In *Figure 8*, we show such plots for isothermal crystallization events in the temperature interval 352–356 K. As can be seen, deviations from the Avrami theory are found at the higher conversion degrees. Deviations from linearity are frequently reported for crystallinities above about 50%. The Avrami equation was initially not developed for macromolecules, but has for polymers been discussed by Wunderlich<sup>10</sup>, Hay and Przekop<sup>16</sup> and Grenier and Prud'homme<sup>17</sup>. It is noted that the Avrami theory may not hold for polymers at the higher crystallization degrees, but a linear relation according to equation (3) is usually found<sup>10,18</sup> at lower conversion degrees. At the fast crystallization at the lower temperatures, we find a linear relationship up to about 70% relative crystallinity, giving Avrami parameters between 3 and 3.5. At the higher temperatures, the deviation sets in earlier, giving a more curve shaped plot, which makes the assessment of the Avrami exponent more difficult. However, we find that the linear part of the data gives similar  $n$ -values of the order 3.5. Thus, we conclude that the  $n$ -values are mainly constant within the narrow temperature range investigated. However, all data imply that a spherical morphology dominates. The half crystallization time ( $t_{1/2}$ ) i.e. the time needed to attain 50% conversion is related to the rate constant  $k$  by the relation  $t_{1/2} = (\ln 2/k)^{1/n}$ . Assuming that the number of heterogeneous nucleation sites are relatively independent of temperature and become active simultaneously, an expression for the temperature dependence of the half crystallization time<sup>18</sup> is deduced from the Lauritzen-Hoffman (LH) theory<sup>11</sup> for polymer crystallization. According to the classical LH-theory, the crystallization is coupled to two independent processes: first, the mass transport across the melt/crystal interface, related to the first exponential in equation (4), and second the formation of a surface or secondary nucleus, as expressed by the second exponential.

$$\frac{1}{t_{1/2}} = C \exp\left(-\frac{U}{R(T_c - T_\infty)}\right) \exp\left(\frac{-K_g}{T_c \Delta T f}\right). \quad (4)$$

In the transport expression, here described with a relation derived from the WLF (Williams Landel Ferry) expression,  $U$  is a constant coupled to the interface transport,  $T_\infty$  is a temperature well below the glass transition where all segmental motions have ceased and  $R$  is the gas constant. The mass transport exponential can be estimated by using

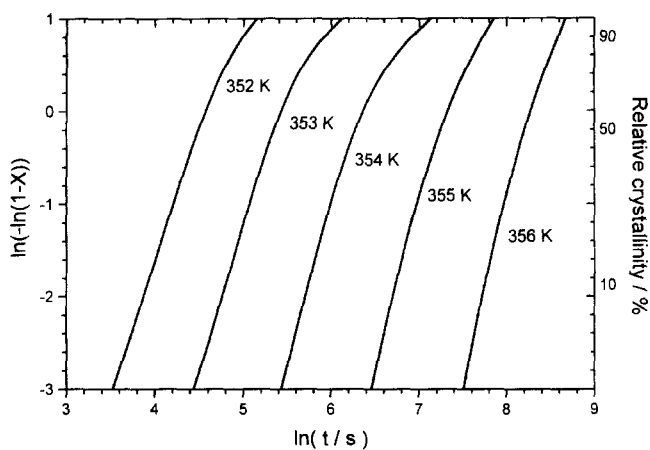


Figure 8 Avrami plots according to equation (3) at isothermal crystallization

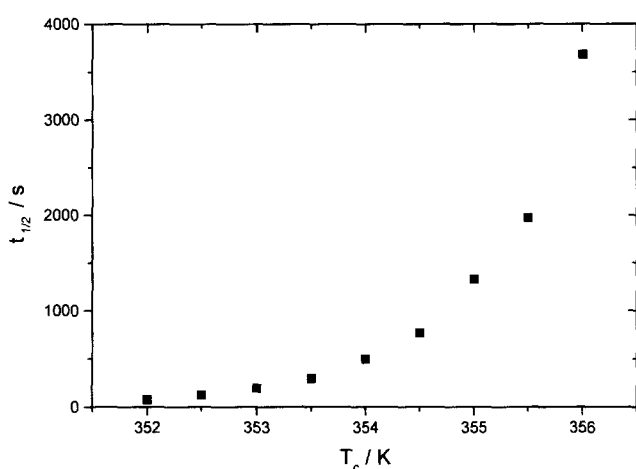


Figure 9 Half time of crystallization versus temperature

Hoffmans<sup>11</sup> 'universal' value of 6280 J/mol for the constant  $U$  and setting  $T_\infty$  to  $T_g - 30$ . In the temperature range investigated here, the growth is controlled by nucleation and the mass transport factor is mainly constant. In the nucleation exponential,  $\Delta T$  is the supercooling and  $K_g$  is the nucleation parameter that contains the ratio of surface energy over lattice energy for the crystal. Finally,  $f$  is a factor that takes the temperature dependency of the heat of fusion into account, usually according to the relation  $f = 2 T_c / (T_c + T_m^\circ)$ . In the LH-model for polymer crystallization<sup>11</sup>  $K_g$  is in the general case written as in equation (5):

$$K_g = j b_0 \gamma \gamma_e T_m^\circ / k \Delta h_m^\circ \quad (5)$$

where  $b_0$  is the thickness of a monomolecular layer,  $\gamma$  and  $\gamma_e$  are the surface energies parallel (the lateral surface) and perpendicular (the fold surface) to the chain axis.  $\Delta h_m^\circ$  is the heat of fusion per unit volume and  $k$  is the Boltzmann constant. Finally,  $j$  is a constant that characterizes the rate at which new chains or nucleus are deposited on the crystal surface. Three different growth regimes have been defined by Hoffman *et al.*<sup>11</sup> In regime I, i.e. at low supercoolings, the linear growth rate normal to the growth front is controlled by the low rate of surface nucleation. In this mono-nucleation regime, the lateral spreading rate is much higher than the surface nucleation rate. Consequently, one surface nucleus causes the completion of the whole substrate, and it

can be shown that  $j = 4$ . In regime II, that is at higher supercooling, the surface nucleation rate increases and multiple surface nucleus are formed and incompleting layers become sites for nucleation. In this polynucleation regime, the linear growth rate is proportional to the square root of the nucleation rate and  $j = 2$ . At even higher supercoolings, the surface nucleation rate increases further and the average distance between the nucleus becomes comparable to the chain width. Thus, there is no time for the lateral growth of the nucleus and the crystallization rate is governed by the surface nucleation and  $j$  is again 4. At lower temperatures close to the glass transition the mass transport will limit the crystallization rate. However, at higher temperatures closer to the melting point it is limited by nucleation. A maximum crystallization rate is reached at temperatures somewhere between these two extremes. The crystallization process of PPDL is clearly nucleation controlled, as the half crystallization time increases with increasing crystallization temperature (see Figure 9). Further, if the secondary nucleation approach is valid, a plot of  $\ln(1/t_{1/2}) + U/(R(T_c - T_\infty))$  versus  $1/(T_c \Delta T f)$  should give a straight line within a given growth regime. The analysis requires knowledge of the equilibrium melting point of the crystallizing component. In the following it is assumed that the molecules capable of crystallization in the investigated temperature range have a similar equilibrium melting temperature of 370 K. In Figure 10 where we show a such plot, we find a linear relation. The extracted slope which is identical to the nucleation parameter  $K_g$  is  $8.7 \times 10^4 \text{ K}^2$ . As indicated above the value of  $K_g$  is quite insensitive to the transport factor and setting  $U = 0$  only changes  $K_g$  to  $8.3 \times 10^4 \text{ K}^2$ . In Table 1 we present collected literature data on the nucleation parameters and some other characteristic data for PPDL and the related polymers PCL and polyethylene. We note that the reported nucleation parameters for PCL varies, between  $4.03 \cdot 10^4 \text{ K}^2$  to  $10.1 \cdot 10^4 \text{ K}^2$ , although the majority of the results can be found within a more narrow range. The values given by Goulet and Prud'homme<sup>14</sup> are mean values between PCL and copolymers of PCL and polymethylcaprolactone, but the value of the nucleation parameter is reported to be independent of the copolymer composition. Further, all authors claim regime II growth. For polyethylene, a value of  $9.55 \cdot 10^4 \text{ K}^2$  is reported by<sup>19</sup> for regime II growth. An estimate of the lateral surface energy for chains with relatively symmetrical cross sections, can be done with the empirical relation,  $\gamma = \Delta h_m^\circ b_0 \alpha$ ,

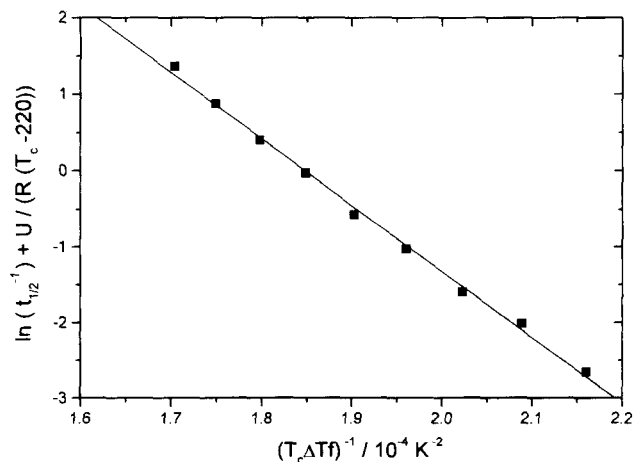


Figure 10 Kinetic analysis of the overall crystallization rate according to the LH theory in equation (4).

**Table 1** Characteristic crystallization parameters for PCL, PPDL and PE

Polymer	PCL			PPDL	PE
Reference	12 <sup>a</sup>	13	14	This work <sup>b</sup>	19
$M_w$	7000, 15 000, 40 000	17 600	48 000	19 400	
$T_m^0/K$	341, 342.5, 343.5	336.7 <sup>a</sup> , 332.3 <sup>b</sup>	347 <sup>b</sup>	370	418.5
$K_g/10^4 K^2$	7.39, 7.33, 8.00	6.71 <sup>a</sup> , 4.03 <sup>b</sup>	9.1 <sup>a</sup> , 10.1 <sup>b</sup>	8.7	9.55
$\gamma_e/10^{-3} J m^{-2}$	87.9, 87.1, 94.7	81 <sup>a</sup> , 49 <sup>b</sup>	106 <sup>a</sup> , 118 <sup>b</sup>	96	93 $\pm$ 8

<sup>a</sup>From optical microscopy<sup>b</sup>From DSC dataThe  $\gamma_e$  values given for PE are established from different methodsThe  $K_g$  and surface energy values given by <sup>14</sup> are mean values for PCL and copolymers between PCL and polymethylcaprolactone

patterned after Thomas and Stavely<sup>20</sup> and discussed by Hoffman<sup>11,19</sup>. Thus, in connection with equation (5) and the nucleation parameter  $K_g$ , the fold surface energy ( $\gamma_e$ ) and the lateral surface energy ( $\gamma$ ) can be separated. According to Hoffman *et al.*<sup>19</sup>,  $\alpha$  is coupled to the chain structure and is close to 0.1 for polyethylene and aliphatic polyesters such as PCL which due to the high number of CH<sub>2</sub> units behave as PE. Here,  $b_0$  is set to 4.12 Å, which is equally to that for PE and PCL<sup>11,12,19</sup>. The resulting value of the fold surface energy for PPDL, assuming regime II growth is 96 mJ/m<sup>2</sup>, which falls within the range that is found for PE of 93  $\pm$  8 mJ/m<sup>2</sup><sup>18,19</sup>. Rego Lopez *et al.*<sup>21</sup> have studied the crystallization of binary blends and pure fractions of polyethylene. They found, that the fold surface free energy for the crystallizing component in the binary blend ( $M_n = 2500$  and  $M_n = 66 000$ ) coincided with the value for the pure, high molecular component. Thus, the nature of the fold surface is mainly independent of the composition of the melt. The value of the nucleation parameter, and thus the fold surface energy, found here is the average value of the molecules capable of crystallization in the investigated temperature range. In a following paper results from a PPDL sample with a more narrow molecular weight will be presented. As seen in Table 1, the values of the fold surface energy for PCL varies from 49 mJ/m<sup>2</sup> to 113 mJ/m<sup>2</sup> and all authors uses regime II growth for the calculations of the surface energy. One explanation for the variance of the fold surface energy for PCL is the different equilibrium melting points, which varies between 332.3 K and 347 K. For example, in our case for PPDL an increase of  $T_m^0$  by 1 K changes the fold surface energy from 96 to 109 mJ/m<sup>2</sup>. The value obtained here for PPDL implies that the work of chain folding is similar to that for PE and thus, that the large number of ethylene units between the COO groups for PPDL give surface properties similar to PE. That is, the number of folds per unit area and the chemical nature of the folds are similar. Further, a change in morphology from axialites in regime I to spherulites in regime II is reported<sup>11</sup> for PE. Phillips *et al.* used regime II growth for PCL because the morphology was spherulitic, in analogy with polyethylene. For PPDL we find a granular appearance for samples both slowly cooled to room temperature and rapidly quenched in liquid nitrogen. This is characteristic for a sample with a large number of heterogeneities acting as primary nucleating centres. The Avrami parameter also indicate that spherulitic morphology dominates, since axialites should give a higher value of the parameter<sup>18</sup>. In analogy with the argument above for PE and PCL, this indicates that regime II growth occurs for PPDL. Further, if we use  $\Delta h_m^0 = 263.7 J/g$  from Wunderlich<sup>9</sup> and a density of 1.2 g/cm<sup>3</sup><sup>22</sup>, i.e. equally to that of PCL, we get a lateral surface energy, of about 13 mJ/m<sup>2</sup> for PPDL. The reported values for PCL are of the order 6–7 mJ/m<sup>2</sup><sup>12,14</sup> and

13  $\pm$  2 mJ/m<sup>2</sup> for polyethylene<sup>18,19</sup>. The results concerning the lateral and fold surface energies imply that the COO groups, separated by the 14 CH<sub>2</sub> groups, do not have any major affect on either the fold surface or the lateral surface.

## CONCLUSIONS AND SUMMARY

Polypentadecanolactone, with its long chain of ethylene units between each COO group, is a fast crystallizing polymer. The crystallization rate is clearly nucleation controlled. The investigated sample has a rather low molecular weight, which in combination with its broad polydispersity, explains the sensitivity to the crystallization temperature at isothermal crystallization. Secondary crystallization also occurs to a significant degree. We find a Hoffman-Week equilibrium melting point of 370 K, and a broad glass transition at about 250 K. In the narrow temperature interval between 352 and 356 K we find fractional Avrami parameters of the order 3–3.5, indicating a spherulitic morphology. Direct observation by optical microscopy of samples slowly cooled to room temperature and rapidly quenched in liquid nitrogen both show a granular appearance characteristic of a large number of heterogeneities acting as primary nucleating centres. By using the Lauritzen-Hoffman crystallization theory and assuming regime II crystallization we find that both the fold surface energy of 96 mJ/m<sup>2</sup> and the lateral surface energy of about 13 mJ/m<sup>2</sup> agrees, within experimental error, with the ones given for polyethylene.

## REFERENCES

- Datta, R., Tsai, S. P., Bonsignore, P., Moon, S. H. and Frank, J.R., *FEMS Microbiology Reviews*, 1995, **16**, 221.
- Pitt, C. G., *Drugs and the Pharmaceutical Sciences*, 1990, **45**, 71.
- Kaloustian, J., Pauli, A. M. and Pastor, J., *Journal of Thermal Analysis*, 1991, **37**, 1767.
- Akahori, S. and Osawa, Z., *Polymer Degradation and Stability*, 1994, **45**, 261.
- Skoglund, P. and Fransson, Å., *Journal of Applied Polymer Science*, 1996, **61**, 2455.
- Richardson, M. J., *Comprehensive Polymer Science*, Vol. 1. Pergamon Press, Oxford, 1989.
- Skoglund, P. and Fransson, Å., *Thermochimica Acta*, 1996, **276**, 27.
- Lebedev, B. and Yevstropov, A., *Makromol. Chem.*, 1984, **185**, 1235.
- Advanced Thermal Analysis (ATHAS)*, Databank of thermodynamic properties of linear macromolecules and small molecules. Copyright Prof B. Wunderlich, Department of Chemistry, University of Tennessee, Knoxville, TN.
- Wunderlich, B., *Macromolecular Physics*, Vol. 2. Academic Press, New York, 1976.
- Hoffman, J. D., Davis, G. T. and Lauritzen, J. I., *Treatise on Solid State Chemistry*, Vol. 3. Plenum Press, New York, 1976.
- Phillips, P.J. *et al.*, *Journal of Polymer Science*, 1987, **25**, 1725.

13. de Juana, R. and Corta'zar, M., *Macromolecules*, 1993, **26**, 1170.
14. Goulet, L. and Prud'homme, R.E., *Journal of Polymer Science*, 1990, **28**, 2329.
15. Wunderlich, B., *Macromolecular Physics*, Vol. 3. Academic Press, New York, 1980.
16. Hay, J. N. and Przekop, Z. J., *Journal of Polymer Science*, 1979, **17**, 951.
17. Grenier, D. and Prud'homme, R. E., *Journal of Polymer Science*, 1980, **18**, 1655.
18. Gedde, U. W., *Polymer Physics*. Chapman and Hall, London, 1995.
19. Hoffman, J. D. et al., *Macromolecules*, 1992, **25**, 2221.
20. Thomas, D. G. and Staveley, L. A. K., *Journal of Chem. Soc.*, 1952, **0**, 4569.
21. Rego Lopez, J. M., Conde Brana, M. T., Terselius, B. and Gedde, U. W., *Polymer*, 1988, **29**, 1045.
22. Wunderlich, B., *Macromolecular Physics*, Vol. 1, Academic Press, New York, 1973.